Electronic properties of III-nitride semiconductors: A first-principles investigation using the Tran-Blaha modified Becke-Johnson potential

Rafael B. Araujo, J. S. de Almeida, and A. Ferreira da Silva

Articles you may be interested in

Ionization potentials of semiconductors from first-principles
J. Chem. Phys. **139**, 164114 (2013); 10.1063/1.4826321

Band gaps from the Tran-Blaha modified Becke-Johnson approach: A systematic investigation
J. Chem. Phys. **138**, 134115 (2013); 10.1063/1.4798706

Electronic structure, vibrational spectrum, and thermal properties of yttrium nitride: A first-principles study
J. Appl. Phys. **109**, 073720 (2011); 10.1063/1.3561499

First-principles investigations of Zn (Cd) doping effects on the electronic structure and magnetic properties of CoFe2O4
J. Appl. Phys. **109**, 07A502 (2011); 10.1063/1.3535442

First-principles calculation of the piezoelectric tensor d of III–V nitrides
Appl. Phys. Lett. **80**, 4145 (2002); 10.1063/1.1482796

Electronic properties of III-nitride semiconductors: A first-principles investigation using the Tran-Blaha modified Becke-Johnson potential

Rafael B. Araujo,[a] J. S. de Almeida,[b] and A. Ferreira da Silva
Instituto de Física, Universidade Federal da Bahia, Campus Universitário de Ondina, 40210-340 Salvador, Bahia, Brazil

In this work, we use density functional theory to investigate the influence of semilocal exchange and correlation effects on the electronic properties of III-nitride semiconductors considering zinc-blende and wurtzite crystal structures. We find that the inclusion of such effects through the use of the Tran-Blaha modified Becke-Johnson potential yields an excellent description of the electronic structures of these materials giving energy band gaps which are systematically larger than the ones obtained with standard functionals such as the generalized gradient approximation. The discrepancy between the experimental and theoretical band gaps is then significantly reduced with semilocal exchange and correlation effects. However, the effective masses are overestimated in the zinc-blende nitrides, but no systematic trend is found in the wurtzite compounds. New results for energy band gaps and effective masses of zinc-blende and wurtzite indium nitrides are presented. © 2013 AIP Publishing LLC. [http://dx.doi.org/10.1063/1.4829674]

I. INTRODUCTION

Over the last decade, the III-nitride semiconductors has emerged as the focus of investigations in many research groups worldwide. The large interest originates from their successful applications in the fields of light-emitting diodes, laser diodes, and high-electron-mobility transistors.[1–3] The reasons for these successful applications are their characteristics such as high temperature stability, very short bond lengths, low compressibility, and high thermal conductivity.[4] A comprehensive study of the electronic properties of III-nitrides became of utmost importance and it has helped to consolidate their wide range of possible commercial optoelectronic applications.

In ambient conditions, III-nitrides display a wurtzite (*wz*) crystal structure[5,6] corresponding to $P6_3mc$ space group. However, these compounds can also crystallize in a zinc-blende (*zb*) cubic structure or NaCl-like rocksalt (*rs*) structure depending on the growth conditions.[4] Currently, the most used theoretical method to study structural and electronic properties of semiconductors is the conventional density functional theory (DFT) using a local or semi-local exchange and correlation functional. It is well known that due to self interaction errors the conventional ground-state Kohn-Sham orbitals are not able to describe satisfactorily some electronic properties. The energy band gaps, for instance, are often too small compared to experimental measurements. Considering that some properties such as energy band gap and effective mass are prerequisites to model electronic devices, it becomes of utmost importance the application of other theoretical methods to find a better description of electronic properties of III-nitride semiconductors.

In this work, we have investigated the electronic structure of AlN, GaN, and InN in both wurtzite (*wz*) and zinc-blend

(*zb*) crystal structures. We carried out DFT-based calculations considering the generalized gradient approximation (GGA) to treat the exchange and correlation term in the Kohn-Sham Hamiltonian. Together with the GGA functional, we have also used a very effective approach to solve the energy band gap problem suggested by Tran and Blaha.[7,8] In this method, the exchange term is treated by the Tran-Blaha modified Becke-Johnson (TB-mBJ) potential and the correlation term is treated within the local or semi-local density approximation in such a way that accurate energy band gaps are predicted. In our calculations, spin-orbit coupling (SOC) effects are included self-consistently to evaluate the band structures of the III-nitrides. It is of great importance to take SOC effects into account because the hole effective masses are strongly dependent on this interaction even when considering the lighter material in this group which is AlN.

Our results for the energy band gap of III-nitrides calculated using the TB-mBJ potential are systematically higher than those obtained using the GGA functional. Additionally, it was found a total discrepancy between band gaps predicted by the TB-mBJ calculations and experimental value of 10% which is much better than the 30% average error found with the GGA functional. Therefore, the TB-mBJ scheme shows an equilibrium between accuracy and the computational time cost which is important for large systems. Furthermore, the TB-mBJ method reveals fairly accurate results for the effective mass of the III-nitrides. This paper will be organized as follows: In Sec. II, we present the theoretical background and the computational details along with the computational parameters used in the calculations. The band structure of AlN, GaN, and InN considering the wurtzite and zinc-blende structures are presented in Sec. III. The effective hole and electron masses are discussed in Sec. IV. Finally, we conclude with a brief summary of the reported results provided by our *ab initio* investigations in Sec. V.

[a]rafaelbna@gmail.com.
[b]jailton_almeida@hotmail.com.

II. COMPUTATIONAL DETAILS

In this work, all calculations were performed using the experimental lattice parameters summarized in Table I. We have performed DFT-based *ab initio* calculations within the full potential linearized augmented plane wave (FP-LAPW) method as implemented in Wien2k code.[9] The exchange and correlation effects were taken into account by using the GGA functional of Perdew, Burke, and Ernzerhof (PBE).[10] Since PBE[11] underestimates band gaps, we have also treated the exchange and correlation effects self-consistently by using the Tran-Blaha modified Becke-Johnson (TB-mBJ) potential.[7,8] This method is a modified version of the Becke-Johnson potential[12] used to improve band gaps obtained by the conventional DFT-based methods. The TB-mBJ potential can be written as

$$v_{x,\sigma}^{TB-mBJ}(\mathbf{r}) = c v_{x,\sigma}^{BR}(\mathbf{r}) + (3c - 2)\frac{1}{\pi}\sqrt{\frac{5}{6}}\sqrt{\frac{\tau_\sigma(\mathbf{r})}{\rho_\sigma(\mathbf{r})}}, \quad (1)$$

where ρ_σ is the electron density, τ_σ is the kinetic-energy and $v_{x,\sigma}^{BR}$ is the Becke and Roussel potential.[13] The c parameter value showed in Eq. (1) is computed with

$$c = \alpha + \beta \left(\frac{1}{V_{cell}} \int_{cell} \frac{|\nabla \rho_\sigma(r')|}{\rho_\sigma(r')} d^3 r' \right)^{\frac{1}{2}}, \quad (2)$$

where V_{cell} means the unit cell volume, $\alpha = -0.012$ and $\beta = 1.023$ borh$^{1/2}$ are parameters fitted according to experimental values.[8] It is important to point out that TB-mBJ is a potential-only functional, i.e., there is no corresponding TB-mBJ exchange-correlation energy. This fact therefore leads to the impossibility of using TB-mBJ to compute Hellmann-Feynman forces and to compare total energies. For the energy which separates valence and core states we used -6 Ry. We also used a sampling of about 1000 $\mathbf{k}$-points in the irreducible Brillouin zone (IBZ) for both crystal structures. The number of plane waves is determined by the product $R_{MT}K_{max}$, where K_{max} is the largest reciprocal vector used in the LAPW basis set and R_{MT} is the *muffin-tin* radius of atomic spheres. In our calculations, we set $R_{MT}K_{max} = 7$ which can be considered a good value for these compounds.

TABLE I. Experimental lattice parameters used in all calculations performed in this paper.

Compound	a, b (Å)	c (Å)	Space group
wz-AlN	3.11[a]	4.89[a]	P6$_3$mc
wz-GaN	3.19[a]	5.18[a]	P6$_3$mc
wz-InN	3.54[b]	5.71[b]	P6$_3$mc
zb-AlN	4.37[c]	4.37[c]	F43$_m$
zb-GaN	4.49[d]	4.49[d]	F43$_m$
zb-InN	4.98[c]	4.98[c]	F43$_m$

[a]Reference 14.
[b]Reference 15.
[c]Reference 16.
[d]Reference 17.

III. BAND STRUCTURES AND FUNDAMENTAL BAND GAPS

The electronic band structures of AlN, GaN, and InN calculated using the experimental lattice constants for both zinc-blende (*zb*) and wurtzite (*wz*) crystal structures using PBE and TB-mBJ methods are shown in Fig. 1. We have chosen to locate the Fermi level at 0 eV and coinciding with the valence band top. It is observed in Fig. 1 that the band dispersions for all compounds look very similar concerning to the method used to treat the exchange and correlation term. The main difference between PBE and TB-mBJ results is a shift factor which increase the energy band gap value systematically in the TB-mBJ calculations. As expected, in the PBE calculations, the valence band maximum appears in the Brillouin zone center at the Γ-point for all electronic band structures. Regarding the conduction band minimum, however, one can notice that the *zb*-AlN reveals an indirect band gap with the minimum of the conduction band located at the X point. For all other compounds a direct band gap was observed. By looking at Fig. 1, it is possible to verify that TB-mBJ method correctly describes the electronic structure of III-nitrides and it reproduces the behavior found in PBE calculations.

The fundamental energy band gap of AlN, GaN, and InN in *zb* and *wz* structures are summarized in Table II. The well known underestimation of its value by the PBE approach is confirmed. We observe a difference of the calculated band gap value within the PBE functional and the experimental value of around 30%. For the TB-mBJ calculations, it shows an average discrepancy comparing with the experimental value of about 10%. Another important point to be emphasized here is that the energy band gap values are reducing along the row AlN, GaN, and InN for both crystal structures independently of the method used to calculate them. One reason to explain this fact is that $5s$ orbital in indium and $4s$ orbital in gallium are lower in energy than $3s$ orbital in AlN, for instance, causing an easy transition of the electrons from the valence band to the conduction band. The existing $p - d$ hybridization in GaN and InN also plays an important contribution to decrease the band gap and, moreover, this effect causes a strong $p - d$ repulsion at Γ point which is not present for AlN leading the *zb*-AlN to an indirect band gap semiconductor with a conduction band minimum situated at the X point.[5]

As discussed above and also by analyzing Table II, one can observe that the TB-mBJ approach has systematically improved the value of the energy band gap obtained by the PBE scheme. This is a result of the addition of a new potential in the Kohn-Sham Hamiltonian.[8] The calculated gap for the *wz*-AlN, for instance, changes from 4.21 eV in the PBE approach to 5.77 eV in the TB-mBJ approach which is much closer to the experimental value of 6.28 eV. The most interesting result of this part of our investigation is the calculation of the energy gap for indium nitride. It is already known that conventional functionals such as PBE predict incorrect results for both *zb*- and *wz*-InN. Experimental results indicate that InN is a semiconductor with energy band gap of 0.7 eV for the wurtzite structure and 0.61 eV for the zinc-blend
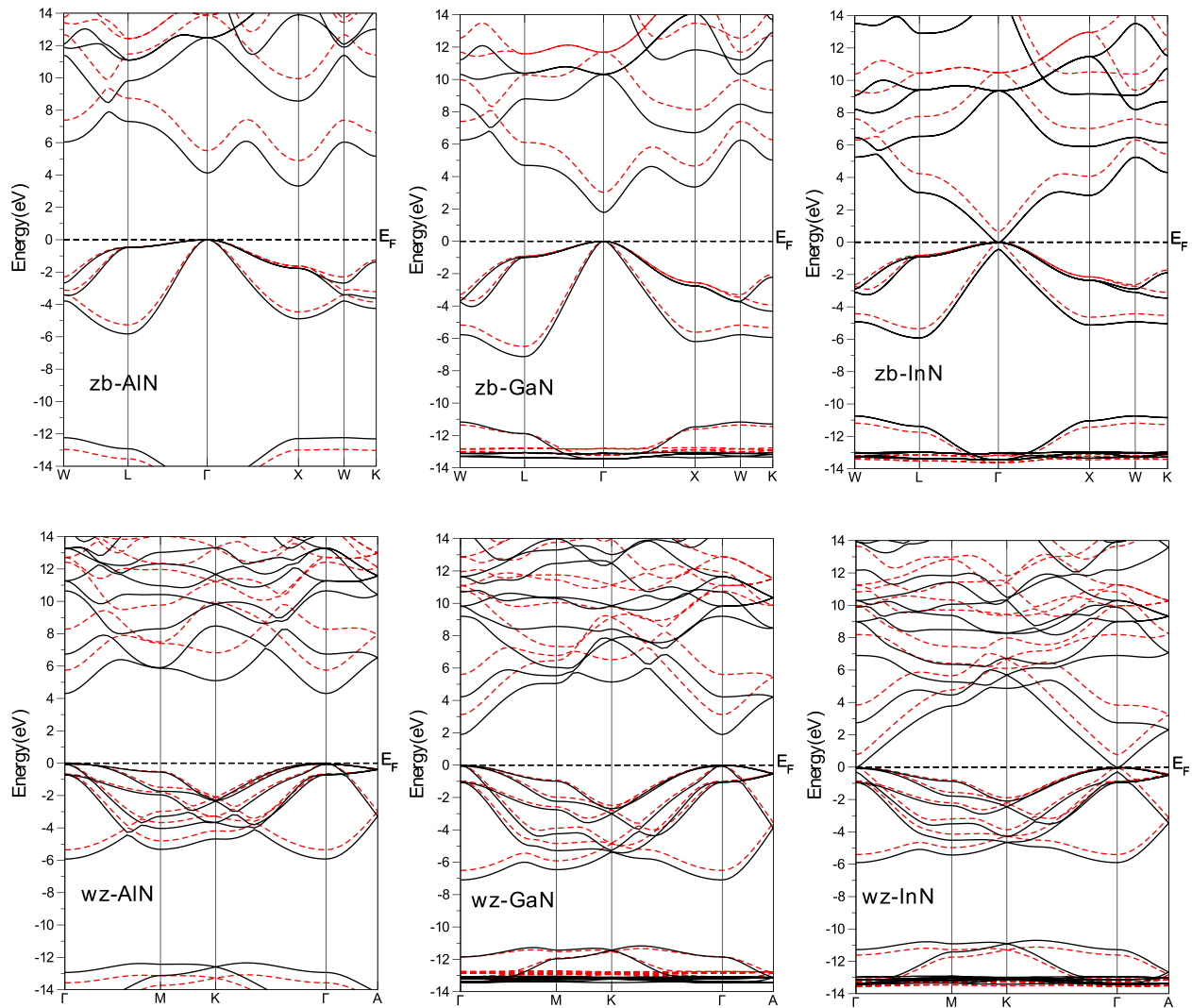
FIG. 1. Electronic band structures of AlN, GaN, and InN in zinc-blende and wurtzite crystal structures. The black full lines represent the calculations with PBE functional and the red dotted lines are representing the calculations with the TB-mBJ method. The Fermi level is shown as a horizontal dashed line.

structure. However, most part of the conventional functionals such as PBE, for instance, predict InN as a metal instead of a semiconductor material forcing one to use more accurate

TABLE II. Comparison between theoretical band gap by using PBE, TB-mBJ, HSE (Heyd-Scuseria-Ernzerhof exchange correlation functional) and G_0W_0 approach on top of HSE ground state calculation, and experimental band gaps (E_g (Exp)), for III-nitrides. The values are given in electron-volt (eV).

Compound	E_g (PBE)	E_g (TB-mBJ)	E_g (HSE)	E_g (HSE+G_0W_0)	E_g (Exp)
wz-AlN	4.21	5.77	5.71[a]	6.14[b]	6.28[c]
wz-GaN	1.79	3.09	3.35[a]	3.37[b]	3.50[c]
wz-InN	…	0.76	0.77[a]	0.49[b]	0.70[c]
zb-AlN	3.20	4.88	4.31[b]	5.16[b]	5.93[d]
zb-GaN	1.67	2.99	2.59[b]	3.16[b]	3.20-3.30[e]
zb-InN	…	0.62	0.206[b]	0.26[b]	0.61[f]

[a]Reference 19.
[b]Reference 5.
[c]Reference 21.
[d]Reference 18.
[e]Reference 17.
[f]Reference 20.

methods such as the computational time expansive GW method to model it. The TB-mBJ appears here as possible alternative to correctly model the energy band gap of InN giving results very close to the experimental ones as showed in Table II at the same computational time cost as the conventional DFT methods. Comparing the band gaps for the III-nitrides calculated using the TB-mBJ with the experimental values we found an average discrepancy of around 10% which is better than the discrepancy obtained using PBE.

IV. EFFECTIVE MASSES

The effective electronic and hole masses are fundamental quantities of the semiconductors, being used in numerous experimental analysis as well as theoretical models.[6] Here, we have calculated the effective masses numerically by fitting the FP-LAPW+SOC band extremes around the Γ point to parabolas. A large number of **k**-points through the high symmetric directions in the reciprocal space was employed and only the nearest ones to the Γ point were taken into account to determine the effective masses. In that sense, we are neglecting non-parabolic effects which could lead to

greater values of the masses.[5] Table III summarizes the results for the III-nitrides in the zinc-blende crystal structure using PBE and TB-mBJ methods. Effective masses were evaluated along the directions [1 0 0], [1 1 0] and [1 1 1] in the *zb* structure. For symmetry reasons in zinc-blende structures, the electronic masses are identical along these directions. Regarding to the *wz* polymorphs the band anisotropy is influenced by the lower crystal symmetry.[5] The curvatures of the bands along the $\Gamma - M$ and $\Gamma - K$ directions are nearly the same, while for the $\Gamma - A$ direction the dispersion becomes different. Table IV shows the results of the effective masses for III-nitrides considering wurtzite crystal structure calculated using the PBE and TB-mBJ schemes.

A. Electron mass in *zb* polymorphs

As mentioned before, the only system which presents an indirect band gap is the *zb*-AlN with conduction-band minimum at the **X**-point. It implies that the electron mass-tensor can be represented by its longitudinal and transverse components ($m_{e\parallel}$ and $m_{e\perp}$). For the *zb*-GaN and *zb*-InN the electron mass is composed just by a single value m_e. The values of $m_{e\parallel} = 0.53\ m_0$ and $m_{e\perp} = 0.32\ m_0$ for the *zb*-AlN calculated in this work using PBE approach show good agreement with the reported in Ref. 5. However, their values calculated using TB-mBJ method which are presented in Table III increase about a factor of 12% for the *zb*-AlN and 25% for the *zb*-GaN in comparison with the PBE values. When comparing the experimental result of the electron mass of the *zb*-GaN with the calculated one it is noticed that the PBE gives a closer value to the measured. Nevertheless, even considering the overestimation of the TB-mBJ method, the numbers given in Table II confirm the extremely small electron

mass of InN observed in experiments. Furthermore, the fact that the TB-mBJ correctly describes the electronic structure of InN allow us to predict its electronic mass using a method that is comparable to PBE in computational cost. Another important feature that turns out to be well described by the TB-mBJ calculations is that the value of electron mass are decreasing along the row AlN, GaN, and InN as it is observed in Ref. 5.

B. Electron mass in *wz* polymorphs

The calculated effective electron masses along the $\Gamma - A$ and $\Gamma - M$ directions to the *wz*-nitrides are presented in Table IV. The lower crystal symmetry of the *wz* structure influences its band anisotropy.[5] Therefore, the curvature of the bands considering the $\Gamma - M$ and $\Gamma - K$ directions are nearly the same, while the $\Gamma - A$ shows a quite different dispersion. The results for the electron masses found here are also in good agreement with the measured values. Comparing it with the experimental one for the electron mass in the $\Gamma - M$ direction for GaN, for example, it is observed an overestimation of around 9% to the PBE functional and 25% to the TB-mBJ method. However, when we analyze the electronic mass of AlN we noticed that both PBE and TB-mBJ show results in the range of the measured value. Another important feature observed in the theoretical calculations is the low value of the electron mass for InN. The difference of the experimental and calculated electron mass in InN is around 20% for TB-mBJ. Such discrepancy, or even bigger, between the calculated and experimental values of the electron mass in InN is also reported by other theoretical works. For instance, Ref. 26 reports an electronic mass for InN in the *wz* as high as 0.14 m_0 which is 100%

TABLE III. Calculated effective masses (in units of the free-electron mass, m_0) for III-nitrides using the PBE and TB-mBJ methods for the *zb* structure. For AlN electron mass case we have included here only the perpendicular effective mass ($m_{e\perp}$). The experimental (Exp) value is also included.

Compound	Functional	m_{hh} (Γ - X)	m_{lh} (Γ - X)	m_{hh} (Γ - K)	m_{lh} (Γ - K)	m_{hh} (Γ - L)	m_{lh} (Γ - L)	m_e (Γ)
zb-AlN								
This work	PBE	1.190	0.450	3.270	0.410	3.660	0.380	0.320
	TB-mBJ	1.400	0.560	3.410	0.490	3.750	0.500	0.360
	HSE[a]	1.320	0.440	2.320	0.390	3.980	0.380	0.300
	LDA[b]	1.440	0.420	3.030	0.370	4.240	0.360	0.280
zb-GaN								
This work	PBE	0.860	0.260	1.880	0.230	1.760	0.300	0.180
	TB-mBJ	0.980	0.440	2.350	0.320	2.040	0.540	0.240
	HSE[a]	0.830	0.280	1.590	0.250	1.950	0.230	0.190
	LDA[b]	0.860	0.210	1.650	0.190	2.090	0.190	0.140
	Exp[c]	…	…	…	…	…	…	0.150
zb-InN								
This work	PBE	…	…	…	…	…	…	…
	TB-mBJ	0.780	0.380	1.080	0.970	0.780	0.300	0.080
	HSE[a]	0.910	0.079	1.550	0.065	1.890	0.070	0.052
	OEPx + G_0W_0[d]	0.840	0.080	1.370	0.078	1.740	0.077	0.054
	Exp[e]	…	…	…	…	…	—	0.040

[a]Reference 5.
[b]Reference 22.
[c]Reference 23.
[d]Reference 24.
[e]Reference 25.

TABLE IV. Calculated effective masses (in units of the free-electron mass, m_0) for III-nitrides using the PBE and TB-mBJ methods for the wz structure. The masses are evaluated along the $\Gamma - A$, $\Gamma - M$, and $\Gamma - K$ directions in the BZ. The experimental (Exp) value is also included here.

Compound	Functional	m_{hh} (Γ - A)	m_{lh} (Γ - A)	m_{SO} (Γ - A)	m_e (Γ - A)	m_{hh} (Γ - M)	m_{lh} (Γ - M)	m_{SO} (Γ - M)	m_e (Γ - M)
wz-AlN									
This work	PBE	3.57	3.07	0.26	0.33	3.39	0.37	4.22	0.32
	TB-Mbj	3.57	2.59	0.27	0.38	1.32	0.37	4.78	0.37
	HSE[a]	3.31	3.06	0.26	0.32	6.95	0.35	3.47	0.34
	…[b]	2.37	2.37	0.21	0.23	3.06	0.29	1.20	0.24
	Exp[c]	…	…	…	0.29-0.45	…	…	…	0.29-0.45
wz-GaN									
This work	PBE	1.70	1.50	0.13	0.21	0.66	0.19	1.12	0.22
	TB-mBJ	1.75	1.65	0.17	0.26	0.56	0.21	0.81	0.27
	HSE[a]	2.00	1.22	0.20	0.21	0.57	0.31	0.92	0.21
	LMTO-LDA[d]	2.00	1.19	0.17	0.35	0.34	0.35	1.27	0.35
	Exp	2.20[e]	1.10[f]	0.30[c]	0.20[c]	0.42[c]	0.51[c]	0.68[c]	0.20
wz-InN									
This work	PBE	…	…	…	…	…	…	…	…
	TB-mBJ	2.08	2.20	0.08	0.09	0.39	0.14	0.31	0.09
	HSE[a]	1.98	1.02	0.08	0.06	0.44	0.09	0.18	0.06
	…[b]	2.44	2.44	0.14	0.14	2.66	0.15	3.42	0.14
	Exp[c]	…	…	…	0.07	…	…	…	0.07

[a]Reference 5.
[b]Ionic model potential, Reference 26.
[c]Reference 23.
[d]Reference 27.
[e]Reference 28.
[f]Reference 29.

greater than the measured value. Following the same rule of the zb polymorphs one can notice a decreasing of the electron masses along the row wz-AlN, wz-GaN, and wz-InN. In general, the electron masses reported in Ref. 5 by using a hybrid functional for these compounds reveals more accurate values. However, such method is really computational time expansive in a way that prevents its usage to model the electronic properties of larger systems.

C. Hole mass in *zb* polymorphs

The calculated effective hole masses of the upmost valence bands for the zb polymorphs are also summarized in Table III. The results calculated using the TB-mBJ method are slightly increased when one compare their values with the results obtained by the PBE functional. However, even considering the greater value of the effective hole mass with the TB-mBJ method the results match relatively well with the values observed in previous works.[5,6,22,23] The overestimation of the effective masses using the TB-mBJ scheme can partly be due to the narrowing of the band widths and we indeed observe that it shows a tendency to localize the valence bands compared to the corresponding PBE results. Additionally, this overestimation can also be a result of the incorrect description of the coupling element between anion-p and cation-s states.[30] The interaction between these states is mainly determined by the hopping integral between the anion p states and the cation s states which is a two center integral. Considering that the TB-mBJ is a pure semilocal potential, it will only act on the one center terms which is responsible for the energy separation between anion-p and cation-s states leading to a overestimation of the effective

masses. The only real problem observed to the effective masses in these calculations with the TB-mBJ potential is relative to the light- hole (lh) in the zb-InN. One can notice in Table III that the results are several times higher than the reported in Refs. 18 and 23. We suspect that this problem is related with the incorrect ordering of the Γ_{1c} and Γ_{15v} levels produced by the PBE calculations[31] and that is not being corrected with the employment of the TB-mBJ framework.

D. Hole mass in *wz* polymorphs

The calculated effective hole masses of the three upmost valence bands for the wz polymorphs are also summarized in Table IV. We can observe that the results considering the TB-mBJ potential to the effective hole masses do not present a systematic behavior as in the zb case in which the TB-mBJ overestimates the effective mass results reported with other methods. By analyzing the wz-AlN, for instance, we are able to notice a good agreement with the values reported in Refs. 5, 22 and the ones obtained by the TB-mBJ scheme. In the case of wz-GaN, the TB-mBJ scheme shows closer results for the heavy-hole (hh) mass than the PBE approach when we compare it with the experimental values. However, the effective mass of the light-hole (lh) depends on the direction considered as one can see in Table IV. This fact clearly explicit that there not exist a systematic trend for the effective mass in wz nitrides using TB-mBJ. In general we could notice that the hole masses are decreasing in the row wz-AlN, wz-GaN, and wz-InN. The value of the hh mass in InN is in good agreement if compared with the showed value in Ref. 5, but it reveals a discrepancy when one compares it with the result from Ref. 22. Such difference might be due to

the accuracy of the band structures and the inclusion of the SOC effects in these calculations. As a whole, the displayed results to the TB-mBJ effective mass in the *wz* structure for the III-nitrides are slightly close to the reported ones in Ref. 5 which uses a hybrid functional to treat the exchange and correlation term. The advantage of the TB-mBJ scheme is its lower computational time cost in comparison with hybrid functional calculations. Another important point to remember, specially in the calculation of *lh* effective mass, is that the choice of the **k**-points region plays a key role to the effective mass due to the non-parabolicity behavior of the band.

V. CONCLUSION

In this paper, we have investigated electronic properties of III-nitride semiconductors by using density functional theory including semilocal exchange and correlations effects through the use of the TB-mBJ method. The band structures, energy gaps, and effective masses near the fundamental band extremes of AlN, GaN, and InN for both zinc-blende and wurtzite crystal structures are calculated. We observe that the inclusion of semilocal exchange and correlation effects systematically increases the energy band gaps of these materials when compared with the results obtained using PBE. The experimental and theoretical energy band gaps present an average discrepancy of about 10% and 30% calculated using the TB-mBJ and PBE methods, respectively. It is important to point out that the TB-mBJ calculations give more accurate energy band gap for these compounds than PBE at the same computational time cost. Regarding the effective masses, we have observed that the TB-mBJ method systematically overestimates their values to *zb* nitrides when comparing them with the PBE calculations while for *wz* no systematic trend is observed for these materials. As a whole the PBE functional presents better effective masses than the TB-mBJ method. Finally, new results for the band gap and effective masses for *zb*-InN and *wz*-InN were derived.

ACKNOWLEDGMENTS

[1] S. Nakamura, S. J. Pearton, and G. Fasol, *The Blue Laser Diode: The Complete Story* (Springer Verlag, Berlin Heidelberg, 2000).

[2] R. Krames, O. B. Shchekin, R. Mueller-Mach, G. O. Mueller, L. Zhou, G. Harbers, and M. G. Craford, J. Disp. Technol. **3**, 160 (2007).

[3] K. Mishra, S. Likun, T. E. Kazior, and Y. F. Wu, Proc. IEEE **96**, 287–305 (2008).

[4] Z. Jiao, S. Ma, and J. Yang, Solid State Sci. **13**, 331–336 (2011).

[5] L. C. Carvalho, A. Schleife, and F. Bechstedt, Phys. Rev. B **84**, 195105 (2011).

[6] C. Persson, A. Ferreira da Silva, R. Ahuja, and B. Johansson, J. Cryst. Growth **231**, 397–406 (2001).

[7] F. Tran, P. Blaha, and K. Schwarz, J. Phys. Condens. Matter **19**, 196208 (2007).

[8] F. Tran and P. Blaha, Phys. Rev. Lett. **102**, 226401 (2009).

[9] P. Blaha, K. Schwarz, G. K. H. Madsen, D. Kvasnicka, and J. Luitz, *WIEN2k, An Augmented Plane Wave + Local Orbitals Program for calculating Crystal Properties*, Karlheinz Schwarz, Techn. Universitat Wien, Wien, Austria, 2001, ISBN:3- 9501031-1–2.

[10] J. P. Perdew, K. Burke, and M. Ernzerhof, Phys. Rev. Lett. **77**, 3865 (1996).

[11] W. Kohn, Phys. Rev. B **33**, 4331 (1986).

[12] A. D. Becke and E. R. Johnson, J. Chem. Phys. **124**, 221101 (2006).

[13] A. D. Becke and M. R. Roussel, Phys. Rev. A **39**, 3761 (1989).

[14] H. Schulz and K. H. Thiemann, Solid State Commun. **23**, 815 (1977).

[15] M. Ueno, M. Yoshida, A. Onodera, O. Shimomura, and K. Takemura, Phys. Rev. B **49**, 14 (1994).

[16] "Properties of group III nitrides," in *EMIS Data reviews series*, edited by J. H. Edgar (IEE INSPEC, 1994), Vol. 11.

[17] H. Landolt and R. Börnstein, *Numerical Data and Functional Relationships in Science and Technology*, (Springer-Verlag, Berlin, 1982), Vol. III, No. 17a and 22a.

[18] M. Röppischer, R. Goldhahn, G. Rossbach, P. Schley, C. Cobet, N. Esser, T. Schupp, K. Lischka, and D. J. As, J. Appl. Phys. **106**, 076104 (2009).

[19] J. Kaczkowski, Acta Phys. Pol. A **121**, 1142 (2012).

[20] J. Schörmann, D. J. As, K. Lischka, P. Schley, R. Goldhahn, S. F. Li, W. Löffler, M. Hetterich, and H. Kalt, Appl. Phys. Lett. **89**, 261903 (2006).

[21] F. Litimein, B. Bouhafs, G. Nouet, and P. Ruterana, Phys. Status Solidi B **243**, 1577 (2006).

[22] L. E. Ramos, L. K. Teles, L. M. R. Scolfaro, J. L. P. Castineira, A. L. Rosa, and J. R. Leite, Phys. Rev. B **63**, 165210 (2001).

[23] P. Rinke, M. Winkelnkemper, A. Qteish, D. Bimberg, J. Neugebauer, and M. Scheffler, Phys. Rev. B **77**, 075202 (2008).

[24] M. Fanciulli, T. Lei, and T. D. Moustakas, Phys. Rev. B **48**, 15144 (1993).

[25] P. Schley, C. Napierala, R. Goldhahn, G. Gobsch, J. Schörmann, D. J. As, K. Lischka, M. Feneberg, K. Thonke, F. Fuchs, and F. Bechstedt, Phys. Status Solidi C **5**, 2342 (2008).

[26] D. Fritsch, H. Schmidt, and M. Grundmann, Phys. Rev. B **67**, 235205 (2003).

[27] K. Kim, W. R. L. Lambrecht, B. Segall, and M. van Schilfgaarde, Phys. Rev. B **56**, 7363 (1997).

[28] J. S. Im, A. Moritz, F. Steuber, V. H. örle, F. Scholz, and A. Hangleiter, Appl. Phys. Lett. **70**, 631 (1997).

[29] M. Steube, K. Reimann, D. Fröhlich, and S. J. Clarke, Appl. Phys. Lett. **71**, 948 (1997).

[30] Y. Kim, M. Marsman, G. Kresse, F. Tran, and P. Blaha, Phys. Rev.B **82**, 205212 (2010).

[31] J. Furthmüller, P. H. Hahn, F. Fuchs, and F. Bechstedt, Phys. Rev. B **72**, 205106 (2005).